JOURNAL OF GEOPHYSICAL RESEARCH, VOL. 115, F03043, DOI:10.1029/2009JF001644, 2010

Models and scales for cross-shore sandbar migration

L. Pape,[1,3] Y. Kuriyama[2] and B. G. Ruessink[1]

Abstract. We investigate the long-term (months to years) predictability of cross-shore sandbar migration with two models that operate on different abstraction levels: (1) a coupled, cross-shore waves-currents-bathymetric evolution model, and (2) two data-driven neural network models, based on simplified cross-shore profile representations and daily-averaged wave properties. For model calibration, training and validation we use a high-resolution 15 year-long profile dataset collected at the Hasaki Oceanographic Research Station in Japan. Sandbar behavior at this field site is characterized by cycles of net-offshore migration with a duration of one to four years. We find that all models can produce several general features of sandbar behavior at the studied field site, such as rapid offshore migration, slower onshore return and net-offshore migration. However, it is difficult to quantitatively predict the offshore-directed trends in sandbar location over timescales of months to years. While simple linear models outperform more detailed nonlinear models, for all models it is difficult to predict long-term sandbar behavior, because of error accumulation in the model's processes over time. Representing processes on a more abstract level (scale aggregation) alleviates error accumulation, but does not completely overcome this problem.

1. Introduction

The cross-shore location of a nearshore sandbar changes over time as a result of the interaction between the sandbar and the incoming waves. Some of the changes in sandbar location are correlated to the temporal variability in wave properties, such as the immediate response to storms, or seasonal trends in sandbar location reflecting the seasonal change in wave height [for a review, see *van Enckevort and Ruessink*, 2003]. However, sandbars may also exhibit trends in their cross-shore location on timescales that are not correlated to the variability in wave climate or other external factors. Some of these trends take place over the course of several months to years, giving rise to quasi-cyclic sandbar behavior. Such cycles typically comprise sandbar generation near the shoreline, a period of net-offshore migration and the eventual decay of the sandbar at the seaward end of the breaker zone. The rate, duration and persistence of net-offshore migration in between sandbar generation and destruction can vary substantially between different sites. Examples of different types of sandbar behavior, ranging from strongly wave-height-driven systems to systems with autonomous trends spanning several months to years, are given in *Lippmann et al.* [1993]; *Wijnberg and Terwindt* [1995]; *Plant et al.* [1999]; *Kuriyama* [2002]; *Aagaard et al.* [2004]; *Certain and Barusseau* [2005]; *Ruggiero et al.* [2005]; *Ruessink et al.* [2003, 2009].

Understanding the processes that give rise to all these types of cross-shore sandbar behavior is a major challenge for researchers working in the nearshore zone. Recent advances in modeling techniques now enable the investigation of long-term (months to years) sandbar behavior with small- and short-scale (meters and up to hours) process-based models. The models of *Ruessink and Kuriyama* [2008]; *Kuriyama* [2009] for example, could reproduce cycles of sandbar generation, offshore migration and decay at the Hasaki Oceanographic Research Station (HORS), Japan, at least in a qualitative sense. These, and other numerical process-based models in general [for an overview, see *Roelvink and Brøker*, 1993], compute hydrodynamics, sediment transport and bottom profile updates over grid cells of decimeters to several tens of meters and timesteps of seconds to hours. Although the equations in such process-based models can describe the underlying processes in great detail, the value of models based on short- and small-scale physical processes for understanding long-term sandbar behavior remains uncertain. Potential problems for this modeling approach are: missing or incomplete descriptions of short- and small-scale processes that turn out to be relevant on larger and longer scales, inaccurate model parameters and error accumulation in the model's nonlinear processes, which might make the model sensitive to its parameters, initial conditions, external forcings and the finite numerical accuracy of the computer running the model. Error accumulation in a model's nonlinear processes can cause exponential divergence between modeled and observed states over time [see e.g. *Lorenz*, 1963]. Even if the representations of the physical processes are highly accurate, error accumulation makes long-term prediction infeasible, and as such, limits the ability to test models and theories about the evolution of long-term sandbar behavior from the short- and small-scale underlying physics.

Other types of models represent sandbar behavior in terms of the more abstract states that the small-scale physics evolve toward. A basic assumption underlying many of the more abstract models is the existence of an equilibrium sandbar location, situated at the cross-shore location of wave breaking [e.g. *Plant et al.*, 1999]. If a sandbar is not at its equilibrium location, the onshore- and offshore-directed sediment-transport processes, such as wave nonlinearity [e.g. *Hoefel and Elgar*, 2003] and undertow [e.g. *De Vriend and Stive*, 1987; *Gallagher et al.*, 1998], drive the sandbar toward that location, until the transports balance and no net sediment transport takes place. If this mechanism indeed drives the sandbar toward a stable equilibrium location, cross-shore sandbar behavior might become easier to predict with models that represent the nearshore zone on the

[1]Faculty of Geosciences, Department of Physical Geography, Universiteit Utrecht, Utrecht, The Netherlands.
[2]Marine Environment and Engineering Department, Port and Airport Research Institute, Yokosuka, Japan.
[3]currently at: IDSIA (Dalle Molle Institute for Artificial Intelligence), Lugano, Switzerland.

0148-0227/11/2009JF001644$9.00

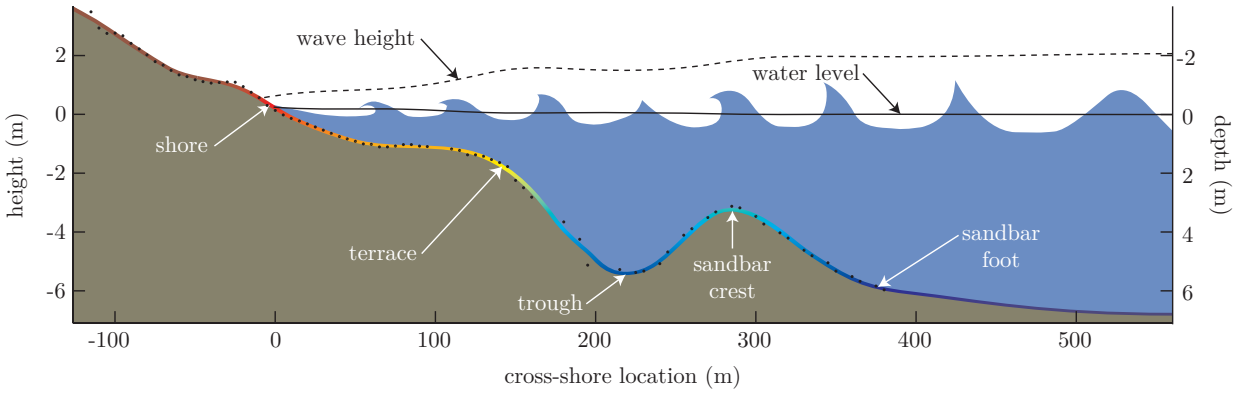

Figure 1. Example of a cross-shore section with a profile in the color scale of Figure 2, sediment in brown and water in blue. The solid (dashed) line indicates the water level (wave height) computed with Unibest.

level of the state a sandbar evolves toward [e.g. *Werner*, 1999, 2003; *de Vriend*, 2001; *Pape et al.*, in press]. Previous analyses and modeling efforts based on this approach can be found in *Plant et al.* [1999, 2001, 2006]; *Pape et al.* [in press].

Where error accumulation limits the prediction of sandbar behavior with small- and short-scale process-based models, long-term trends might better be understood with the help of models that represent sandbar behavior in terms of more abstract states. In this work we investigate how the capacity to predict long-term cross-shore sandbar behavior is affected by the abstraction level on which a model represents the nearshore zone. Here, cross-shore sandbar behavior refers to the change in the cross-shore location of a sandbar as a feature, not the change in shape or volume (e.g. sandbar generation or decay). We compare two models that operate on different spatial and temporal scales: (1) the Unibest model [*Ruessink et al.*, 2007], which computes wave-averaged equations of hydrodynamics and sediment transport over a cross-shore transect of the nearshore, and (2) a data-driven Nonlinear AutoRegressive neural network with eXogenous inputs (NARX) [*Rumelhart et al.*, 1986; *Pape et al.*, 2007], which models simplified profile representations comprising one up to three coordinates of relevant changes in profile slope, and daily-averaged wave properties. Both Unibest and NARX are *iterative* models, i.e. they update the variables that represent the profile or sandbar state in a stepwise fashion, using previously predicted profile or sandbar-state variables and observed hydrodynamic conditions as inputs. The main difference between the two models is the abstraction level on which they operate. Unibest represents the nearshore zone as a series of profile elevations over a cross-shore transect, and involves no a priori notion of a sandbar. The neural network models, on the other hand, assume the presence of a sandbar and describe several aspects of its cross-shore evolution. Note that the comparison between Unibest and NARX is not meant as a practical contest between a process-based and a data-driven modeling paradigm, but is performed here to investigate fundamental aspects of the predictability of cross-shore sandbar behavior.

The data used for model calibration, training and validation is a 15 year-long high-resolution dataset of in situ profile observations from the Hasaki Oceanographic Research Station (HORS) in Japan. This unique dataset is both dense and extensive in space and time and covers several cycles of net-offshore migration. It thus enables us to perform a detailed investigation of the differences between the process-based Unibest model and the more abstract NARX model.

2. Observations

An extensive beach profile dataset was collected between January 1987 and December 2001 at the Hasaki Oceanographic Research Station (HORS), Japan [*Kuriyama*, 2002]. During this period, profile measurements were taken from a 427 m-long pier at 5 m intervals each week-day. The HORS research facility is located near the city of Kashima, in the center of a 17 km strip of sandy coast facing the Pacific Ocean. The beach at the study site is enclosed by the 3 km-long breakwater of the Kashima Port in the north, and the 1 km-long breakwater of the Hasaki Fishery Harbor at the southern side. The profile slope in the sandbar zone is 1 : 125 and the grain size is 180 μm. Tides at HORS are semi-diurnal, with a range of 0.7 to 1.4 m. The average wave height at the Hasaki coast is 1.2 m. Waves are usually larger from autumn to spring than during the summer months, owing to depressions in winter and spring, and typhoons during autumn.

A timestack plot of the collected profile data is given in Figure 2a. As can be inferred from this figure, two sandbars located between 100 – 150 m and 160 – 400 m from the shoreline are usually present in the submerged part of the nearshore zone. Here, the sandbar closest to the seaward end of the pier is referenced as the outer sandbar, while the next shoreward-located sandbar is called the inner sandbar. The sandbars at HORS exhibit trends of net-offshore migration over the course of one to four years. At the beginning of the migration cycle, a sandbar is generated near the shoreline. After that, the sandbar travels mainly in the offshore direction until it reaches the seaward end of the breaker zone situated at the tip of the pier. Sandbar decay usually sets in after the typhoon season and is followed by the offshore migration of the existing inner sandbar, which then becomes the new outer sandbar. While at HORS the net trend in sandbar migration is always offshore (i.e. sandbars are created at the shore and destroyed at the seaward end of the breaker zone), during long periods of low-energy conditions the sandbars sometimes migrate back onshore for a while, extending a sandbar's lifetime [see also *Kuriyama et al.*, 2008].

Although the inner sandbar is referenced as a bar here, it mostly resembled a terrace-like feature that was not clearly separated from the shoreline by a shoreward-located trough (for an example, see Figure 1). Bathymetric surveys in a 600 m-wide area centered on the pier revealed that the inner sandbar often develops crescentic features and rip channels, while the outer sandbar remains alongshore uniform [*Kuriyama*, 2002]. Because of the alongshore variability in the inner sandbar, profiles taken over a single cross-shore transect cannot be used to accurately define the location of the inner sandbar. Therefore, we restrict our modeling efforts to the outer sandbar in the remainder of this paper.

We divided the profile data into time-periods starting with the transition from inner to outer sandbar (i.e. outward migration after decay of the former outer sandbar) up

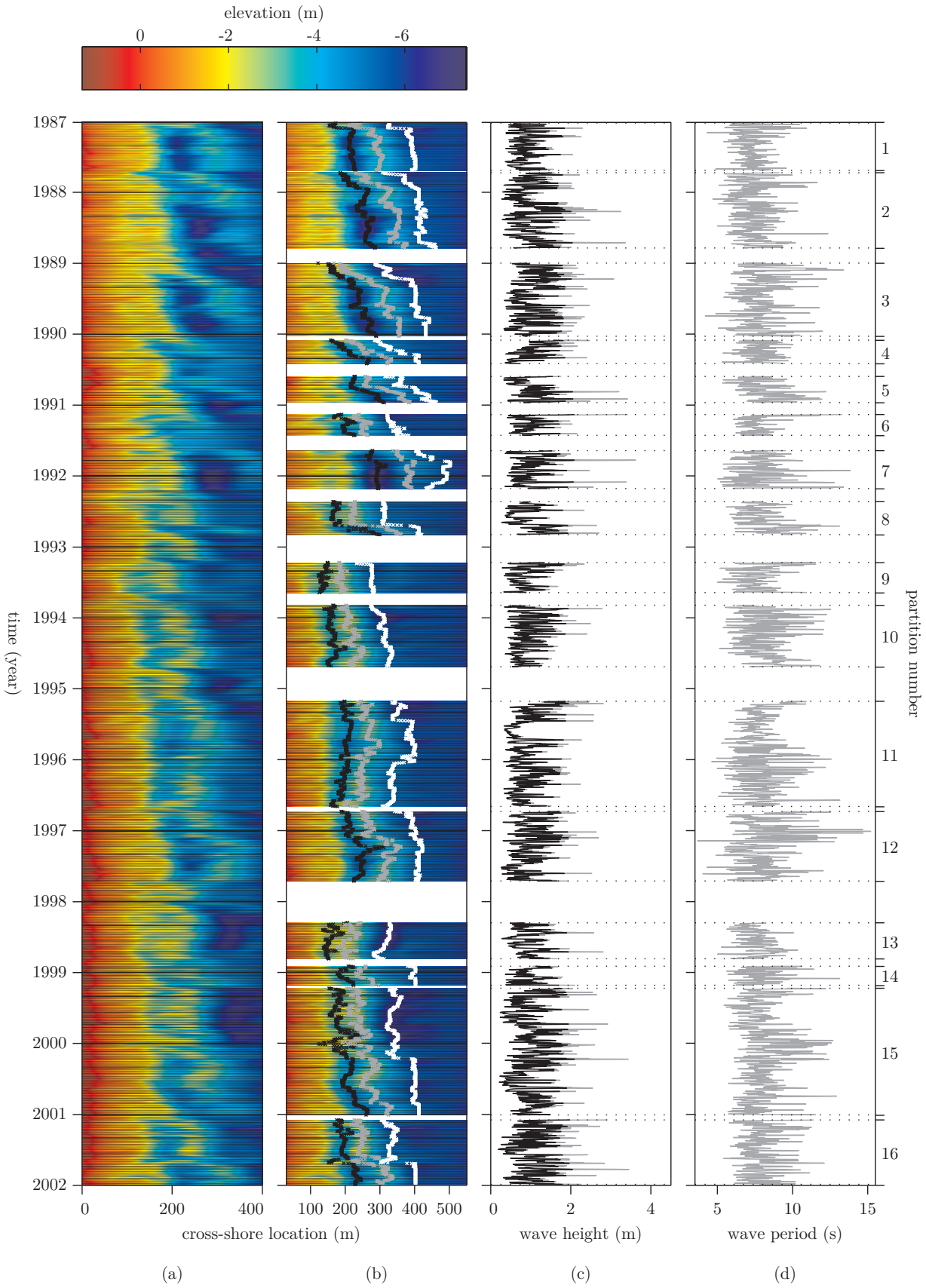

Figure 2. HORS observations: (a) original profile observations; (b) extended profiles divided in partitions of continuous sandbar presence with trough (black), sandbar-crest (gray) and sandbar-foot (white) locations; (c) offshore-measured (gray) and local (black) root-mean-squared wave heights; (d) offshore-measured peak wave period. Each partition contains one offshore migration cycle of the outer sandbar.

to the end of a sandbar's life (i.e. complete decay, or migration beyond the tip of the pier). This yielded 16 partitions of continuous outer sandbar presence (see Figure 2b), containing a total of 3106 days of profile observations. From each of these profiles we extracted three coordinates that indicate the state of the outer sandbar: (1) the sandbar crest, defined as the local maximum elevation at the seaward side of the profile, (2) the landward trough, defined as the local minimum elevation at the landward side of the sandbar crest and (3) the sandbar foot, defined as the slope break at the seaward side of the sandbar crest (see Figure 1). The resulting time-series of trough, sandbar-crest and sandbar-foot coordinates are depicted in Figure 2b. In the following, we use the cross-shore location of the sandbar crest to indicate the cross-shore location of the sandbar as a feature, and express model performance of sandbar migratory behavior in terms of differences between observed and model-predicted sandbar-crest locations.

Wave height and period data were measured at the Kashima Port ultrasonic wave gauge (located 5 km offshore in 24 m water depth), and averaged over one day. Since no detailed directional wave information was available from this, or nearby wave gauges, the average absolute wave direction of 30° (relative to the shore normal) over this part of the Japanese coast was used when necessary. Also, no in situ water level observations were available, so the hourly-computed astronomical tidal level was used instead when required. Local wave heights were computed with the Battjes-Janssen wave transformation model [*Battjes and Janssen*, 1978; *Battjes and Stive*, 1985] at a fixed point 50 m offshore of the seaward end of the sandbar zone, where the waves are not yet affected by the presence of the sandbar. This procedure is explained in detail in *Pape and Ruessink* [2008]. The time-series of offshore-measured and locally-computed wave heights are depicted in Figure 2c, and the time-series of offshore-measured wave periods are given in Figure 2d.

3. Models

3.1. Unibest

Unibest is a wave-averaged, coupled, waves-currents-bathymetric evolution model for cross-shore profiles in the submerged part of the nearshore zone. Starting from an initial observed profile and known offshore wave and tide conditions, Unibest updates the profile with the computed bed-level changes over a certain time interval. The updated profile is used in the next timestep in the calculation of the hydrodynamics, sediment transport and bed-level changes. Offshore sandbar migration in Unibest is the result of interaction between the sandbar, wave breaking, undertow, and suspended sediment transport, while onshore sandbar migration results from feedback between near-bed wave skewness, bedload transport, and the sandbar. The details of Unibest's hydrodynamic and sediment-transport models are described in *Ruessink et al.* [2007]. Because of the capacity of Unibest to model both onshore migration [*Ruessink et al.*, 2007] and net-offshore migration over several months [*Ruessink and Kuriyama*, 2008], we here use Unibest to represent the class of models that base their computations on the short- and small-scale physical processes. In Section 5 we will argue why the outcome of the experiments we perform here is not specific for the choice of Unibest, but can be generalized to all instances in this class of models.

The cross-shore domain represented in Unibest ranged from the dune foot 100 m onshore of the waterline to the location of the wave gauge 5 km offshore. The part of this domain that was not covered by the daily pier observations was filled with the long-term average profile up to 700 m from the shore, and a linear slope (about 1 : 250) from 700 m to 5 km offshore. Since the outer sandbar hardly ever migrates seaward of the pier [*Kuriyama*, 2002], the long-term average profile seaward of the pier will not deviate much from the actual profiles over that part. The model domain was divided into grid cells ranging in size from 100 m in deep water to 1 m in the sandbar areas. A variable timestep was used, with a target value of 6 hours and a minimum of 45 minutes. When the bed-level change at any cross-shore location exceeded 5 cm, the timestep was reduced until the bed-level change became smaller than 5 cm or the timestep reached the minimum allowed value of 45 minutes. The variable timestep reduced the computational time considerably with respect to the constant timestep of 1 hour used by *Ruessink et al.* [2007], while yielding virtually identical results. The forcing variables for Unibest consisted of hourly-computed astronomical tides and daily-averaged root-mean-squared wave heights, peak wave periods and wave direction. At the start of each partition (see Figure 2), the observed profile was supplied to Unibest, after which the model was iterated forward with hydrodynamic variables and predicted profiles. Profile predictions were read out at timesteps corresponding to the observation times.

The Unibest model has a number of adjustable parameters that need to be calibrated to a specific study site. Here we used several sets of parameters: (1) parameter settings obtained by *Ruessink et al.* [2007] on the first 44 days of the HORS dataset, and (2) parameter settings obtained by a calibration procedure based on the Nelder-Mead simplex method [*Lagarias et al.*, 1998]. The Nelder-Mead simplex method searches the parameter space using the profile-elevation error of Unibest runs as objective function. Coordinates in the parameter space that are to be evaluated are efficiently selected by extrapolating the behavior of the objective function. Following *Ruessink et al.* [2007], we limited the Nelder-Mead calibration to the current-related roughness k_c [*van Rijn*, 1993], the scale factor for the vertical eddy viscosity distribution function in the undertow model α_w [*Reniers et al.*, 2004], and the maximum angle of a stable slope $\tan(\phi)$ [*Roelvink et al.*, 1995], also called the angle of repose. *Ruessink et al.* [2007] showed that the effect of bounded long waves on the net sediment transport rate is insignificant in the Unibest model, so a fourth parameter c_r, representing the effect of long waves, was left at its original *Ruessink et al.* [2007] value. The search space of the simplex method was limited by setting bounds outside which the parameter values would not be physically realistic, using the values in Table 1.

Calibration was performed for each partition individually, using one up to fourteen neighboring partitions. For example, the eight neighboring partitions of partition 1 are partitions 2 to 9, and the four partitions neighboring partition 2 are partitions 1, 3, 4 and 5. The partition under study is thus excluded from the calibration algorithm, and will be referred to as the test partition in the following. For each parameter combination selected by the simplex method, Unibest was run on the selected neighboring partitions. Calibration errors were defined as the root-mean-squared error in profile-elevation between the 30 and 550 m-coordinate (Figure 2b), which covers the barred part of the nearshore zone. Using a value of 375 m for the seaward edge of the calibration domain as was done in *Ruessink et al.* [2007], yielded uncontrolled sandbar behavior beyond the tip of the pier, because that part is not included in the error computation. Although the daily profile observations range only to the tip of the pier at the 400 m-coordinate, extending the range 150 m beyond the pier forced sandbar decay for sandbars entering that area. Errors were averaged over the selected neighboring partitions, and days for which no observations were available were neglected in the error computation. We found that using two neighboring partitions for calibration yielded the best performance on the test partitions. A more detailed

discussion of the effect of using different numbers of neighboring partitions for calibration is given in Section 4.1. To verify the reliability of the Nelder-Mead parameter search, we repeated 20 randomly selected calibration runs with a grid search (8000 grid cells) within the parameter bounds of Table 1. For all trials, the Nelder-Mead results were found in the optimum of the parameter search grid.

3.2. Neural networks

Instead of solving the details of undertow, wave nonlinearity and sediment transport, models can also be represented on the level of the patterns that emerge from the underlying processes. In such a more abstract representation, sandbars can be described with only a few variables, such as the cross-shore location of the sandbar crest, or the parameters of a Gaussian curve superimposed on a linear sloping profile [*Plant et al.*, 2001]. While these abstract representations can — at least conceptually — be linked to the underlying physics [see e.g. *Plant et al.*, 2001; *Pape et al.*, in press], no equations are known that describe the relation between wave properties and abstract representations of the sandbar state, such as sandbar location, shape and crest-depth. Nevertheless, it is possible to derive the relation between abstract sandbar-state variables and wave properties from observations with the help of a data-driven model. Data-driven models can be considered as black-box models in the sense that the correlations they find are often not easily understandable. However, the focus of this work is not to find an intelligible model for sandbar behavior, but merely to investigate how the abstraction level of a model affects the predictability of long-term sandbar behavior.

Earlier work done by *Pape et al.* [2007] showed that a neural network is able to predict sandbar behavior on timescales of months to years. Moreover, it is known that such a neural network can estimate *any* function with arbitrary precision [*Hornik et al.*, 1989]. As such, a neural network will be able to model the — as yet unknown — function that describes how sandbars behave on a more abstract level. Because a neural network is the most general instance of the class of models that describe sandbar behavior on any abstraction level, we will here use a neural network model to investigate predictability of sandbar behavior based on simplified representations of cross-shore profiles. A neural network [e.g. *Bishop*, 1995] consists of a collection of interconnected nodes that exchange signals. Signals enter the network at the input nodes, and travel through the network to the output nodes. Each node applies a certain transfer function to its input values, while connections modify the signals they carry with a certain weight. A neural network can be trained to produce certain activation patterns in the output nodes, given the inputs, by adjusting the weights of the connections. After the training procedure is carried out repeatedly (each repetition is called an epoch) on a certain part of the observations, called the training data, the network's generalizing capacity can be tested on parts of the data that were not used during training.

The neural network used here is based on the NARX recurrent neural network architecture used by *Pape et al.* [2007]. Recurrent neural networks, in contrast with often-used feedforward neural networks, can use the temporal structure in their inputs to optimize the output signal. We investigate two NARX models with different representations of a sandbar's cross-shore state: (1) the cross-shore sandbar-crest location (similar to *Pape et al.* [2007]) and (2) the coordinates (cross-shore and vertical) of the trough, the sandbar crest and the sandbar foot (see Figures 2b and 1). For the sandbar-location representation we created a NARX model with one output node for the sandbar location, an input node for the wave height, and an additional recurrent input connection from the output node, representing the sandbar location predicted at the previous timestep. For the three-coordinate representation we used a network with six output nodes for the trough, sandbar-crest and sandbar-foot coordinates (cross-shore and vertical), two input nodes for the wave height and period, and six additional recurrent input connections from the output nodes, representing the predicted coordinates at the previous timestep. In the sandbar-crest-based model no depth information is available, so the local wave height and the water depth above the sandbar crest, which are important for determining the direction and rate of sandbar migration, can only be roughly estimated from the cross-shore sandbar location. The more detailed three-coordinate-based neural network, on the other hand, can form internal representations of a sandbar's cross-shore shape, volume, and crest-depth, and the local wave properties when necessary. As such, we provided locally-computed wave heights to the sandbar-crest model and offshore-measured wave height and period data to the three-coordinate model. The wave direction is assumed constant over the dataset, so it was not used as input to the neural networks. Both neural networks operated with a fixed timestep of one day, and were driven forward with daily-averaged wave information.

The training method used for the NARX neural network was the backpropagation through time (BPTT) algorithm [e.g. *Williams and Peng*, 1990]. BPTT collects the errors and unfolds the network over a certain amount of timesteps, called the batch size. Because the training procedure can be sensitive to the choice of batch size [for an explanation, see *Pape et al.*, 2007], the batch size was varied each epoch by selecting a random value between 2 and the total amount of samples in each partition. A bold driver algorithm was used to automatically determine the learning rate parameter. This algorithm increased the learning rate each batch by one percent, until the error increased more than 0.1 percent of the target range compared with the previous minimum error. In that case, the learning rate was dropped by 25 percent, and training was resumed from the weight settings that produced the minimum error. Input data were normalized between -1 and 1 before presentation to the network, and re-scaled to the original values before error computation. Since the timestep of the neural network corresponds the resolution of the observations (i.e. one day), errors could be computed at each timestep. Days at which no observations were available were skipped in the error and weight-update calculations. Training was performed until the error converged, which generally happened around the presentation of 10^9 samples to the network.

Similar to the Unibest calibration procedure, neural networks were trained for each partition, using a certain number of neighboring partitions. Since neural networks are data-driven models, they generally need more data to reliably extract the dynamics than process-based models. However, we found that using more than eight neighboring partitions during training did not result in improved performance on the test partitions for both the sandbar-crest and the three-coordinate model. As such, all further neural network experiments were performed using eight neighboring partitions for training.

We performed a number of trials to determine the optimal network size with networks containing 0 up to 20 hidden nodes with hyperbolic tangent transfer functions, organized in zero to two hidden layers. During training we tested for overfitting (the neural network starts to learn the specifics of the training data (noise) instead of the general aspects) on the partitions not used for training or testing, called validation partitions. We found that the error steadily converged to a minimum on the validation sets, probably because the training dataset was sufficiently large and the networks were sufficiently small to prevent overfitting. For both the sandbar-crest-based model and the three-coordinate model,

Table 1. Parameter values for the Unibest model. Standard deviations over the 16 partitions are given between parentheses, and where convenient, as percentages of the mean values.

	k_c (m)	α_w	$\tan(\phi)$
calibration search range	0.005 – 0.08	0.02 – 0.2	0.005 – 0.3
Ruessink et al. [2007] parameters	0.037	0.056	0.141
calibration on 1 partition	0.029 (71%)	0.13 (46%)	0.15 (63%)
calibration on 2 partitions	0.026 (63%)	0.13 (43%)	0.15 (68%)
calibration on 8 partitions	0.011 (55%)	0.17 (20%)	0.12 (81%)

a network without any hidden nodes (i.e. a linear network) outperformed networks with hidden nodes (i.e. nonlinear networks) for prediction horizons of several months. We therefore used a linear model with recurrent training for both the sandbar-crest and the three-coordinate representation in all further experiments. Although these models are both *linear* models, the recurrent training procedure is not equivalent to linear regression, since the error is minimized over the iterative result of all batch sizes, and not over individual samples. For an in-depth discussion about the increased performance of linear over nonlinear models, see *Pape et al.* [in press]. In the following, we will refer to the sandbar-crest-based model as RLARX-C (Recurrent Linear ARX for sandbar-Crest) and to the three-coordinate representation as RLARX-3P (Recurrent Linear ARX for 3 Profile coordinates).

4. Results

For each of the 16 partitions, the calibration and training procedures described in the previous section were carried on the neighboring partitions. Next, the optimal parameters found for the partitions neighboring the partition under study were used to compute model outputs for that partition. The predicted profiles for the Unibest runs with the parameters from *Ruessink et al.* [2007] are depicted in Figure 3a. The profiles of the Unibest runs using the parameters obtained with the Nelder-Mead calibration method for two neighboring partitions (best results) are given in Figure 3b. Additionally, Unibest predictions with parameters calibrated on eight neighboring partitions (same as neural network training procedure) are given in Figure 3c. As becomes clear from Figure 3 the Nelder-Mead-calibrated Unibest runs sometimes produced profiles without well-developed sandbars (compare for example partition 7 in Figures 3a and 3c). To allow sandbar-crest extraction from such profiles, we posed additional constraints on the sandbar-crest extraction algorithm. In case sandbar decay took place before the end of a partition, the first slope break counted from the seaward side was taken by the extraction algorithm as the location of the sandbar. If no slope break could be found in a profile, the extracted sandbar location from the previous day was used. In this fashion, the sandbar locations produced by the algorithm stayed in place even after complete sandbar decay, so error measures could still be computed for sandbar-less profiles. The extracted sandbar locations for the Unibest runs are plotted on top of the profiles in Figure 3.

The parameter settings from *Ruessink et al.* [2007] and the average of the optimal parameter values found by the calibration procedure are given in Table 1. Note that the calibration procedure was performed for each partition (on the selected neighboring partitions), yielding 16 different combinations of optimal parameters. Apart from the average of the optimal values, Table 1 also gives the standard deviations of the parameters over the 16 partitions.

The time-series of sandbar locations predicted by the RLARX-C model are depicted in Figure 4a, and the RLARX-3P results are given in Figure 4b. To give an indication of the predicted sandbar-crest elevation and the predicted locations and elevations of the sandbar-foot and trough of RLARX-3P, we reconstructed profile data from the predicted coordinates and the time-average (sandbar-less) profile over the partitions used for training. At each timestep, a profile was created using the three predicted coordinates in the cross-shore range between the predicted sandbar-foot and trough, and the elevations of the mean-observed profile outside of this range. The resulting profiles were interpolated to the observed profile grid with monotone cubic interpolation [*Fritsch and Carlson*, 1980]. Figure 4b shows the profiles that were constructed in this fashion in the same color scale as Figure 3.

We computed root-mean-squared errors (RMSE) between observed and predicted sandbar locations for all timesteps at which observations were available. The RMSE values together with their standard deviations over the 16 partitions are given in Table 2. Apart from the RMSE measure, we calculated skill scores to indicate a model's performance relative to a baseline prediction of no change since the first sandbar-crest observation in a partition. Skills were calculated over each partition as:

$$\text{skill} = 1 - \frac{e_\text{p}}{e_\text{b}}, \tag{1}$$

where e_p is the root-mean-squared difference between model-predicted and observed sandbar locations, and e_b is the root-mean-squared difference between the baseline and the observations. According to this formulation, positive skill scores indicate that the model prediction is better than the baseline prediction of no change, zero skill means the model's performance is equal to the baseline prediction, and negative skill scores imply that the model performs worse than the baseline. The average skill scores together with their standard deviations over all 16 partitions are given in Table 2. For comparison, Table 2 also includes performance measures of the long-term mean sandbar location based on the eight neighboring partitions of each predicted partition.

4.1. Unibest

As becomes clear from Figure 3, Unibest was able to reproduce several general features of sandbar behavior, such as rapid offshore migration (e.g. Figures 3a and 3b in partition 3) and onshore migration (Figures 3a and 3b in parts 12 and 13). Furthermore, cycles of sandbar creation and decay were sometimes generated by Unibest (e.g. Figure 3a in partition 11). However, Unibest struggled to predict sandbars at the right location, despite our efforts to optimize its parameter settings.

Using parameters from *Ruessink et al.* [2007], Unibest was unable to outperform both the baseline prediction (negative skill) and the long-term mean sandbar location (see Table 2). Figure 3a reveals that this is mainly because the predicted sandbars migrated seaward at a much faster rate than the observed sandbars (e.g. in partitions 3 and 16).

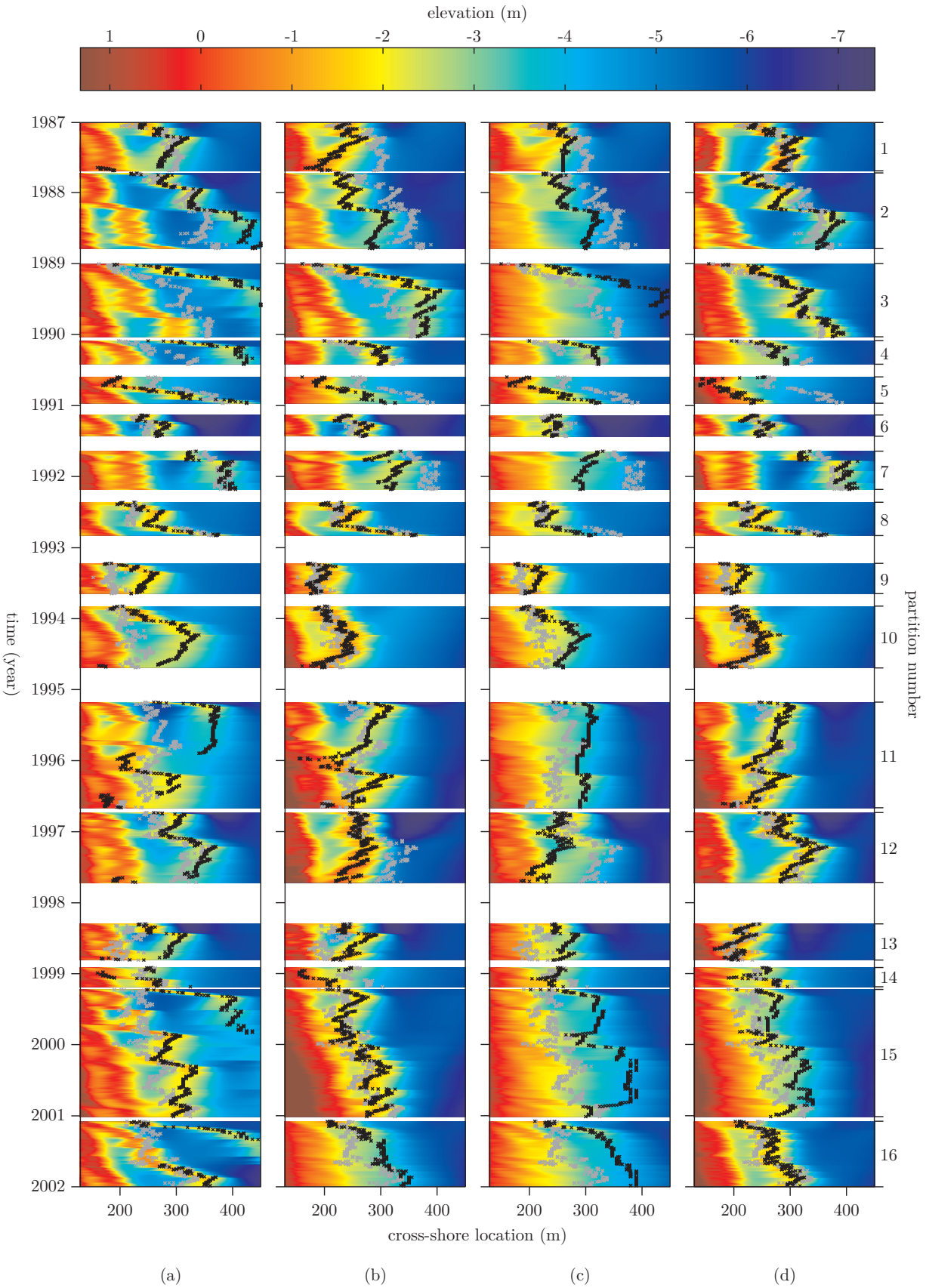

Figure 3. Model predictions: (a) Unibest results obtained with the *Ruessink et al.* [2007] parameters; (b) Unibest results obtained from calibration on 2 neighboring partitions; (c) Unibest results obtained from calibration on 8 neighboring partitions; (d) Unibest results obtained from calibration on the hindcasted partition. Predicted (observed) sandbar locations are indicated in black (gray).

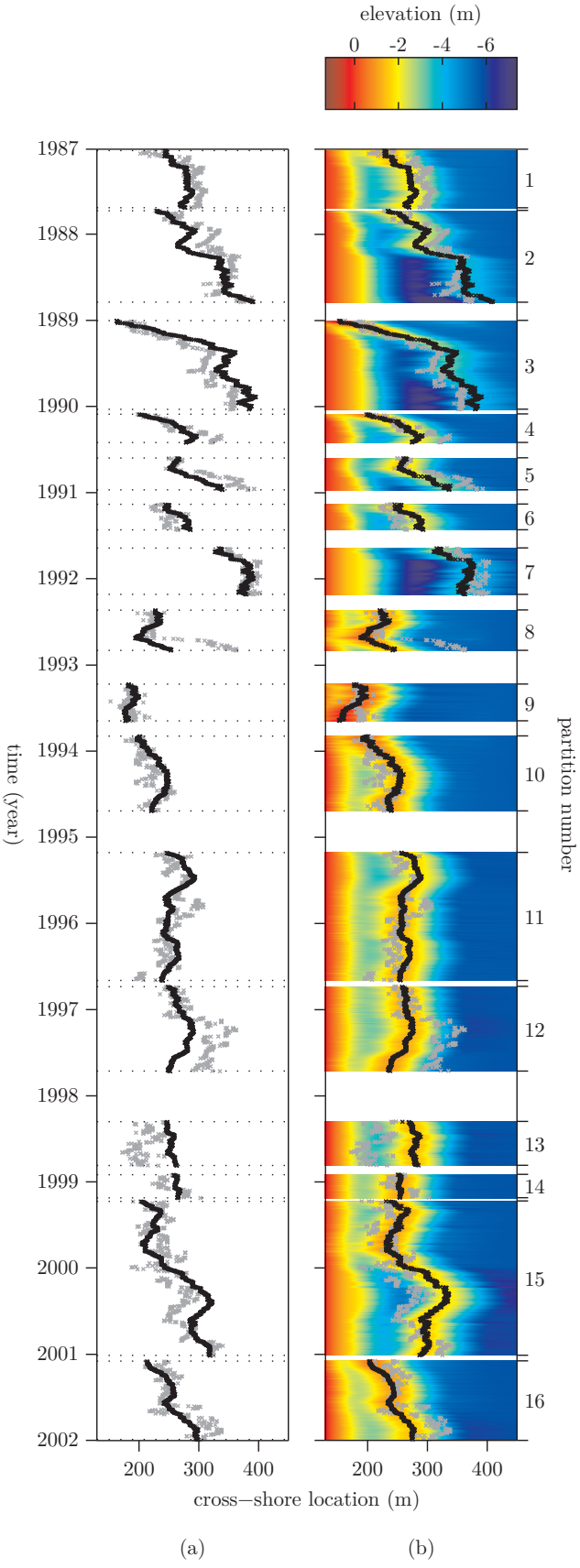

Figure 4. Neural network predictions (black) and observations (gray) for: (a) RLARX-C; (b) RLARX-3P embedded in the long-term mean profile.

Since the predicted sandbars would not decay when migrating beyond the tip of the pier, the differences between observed and predicted profiles became increasingly larger near the end of each partition. Even though Unibest accurately predicted offshore and onshore sandbar migration in some parts of the data (e.g. in partition 1), most of the time the predicted offshore migration rate was wrong, yielding an overall negative skill score with a large standard deviation.

The parameters obtained with the Nelder-Mead calibration method on two neighboring partitions yielded the best Unibest prediction performance (Figure 3b and Table 2). However, to achieve this performance, rather different parameter settings for different partitions were needed (large standard deviation in Table 1). For some partitions the Nelder-Mead calibration method found parameters settings that resembled those found by *Ruessink et al.* [2007], but for other partitions completely different optimal settings were found, sometimes even close to the upper limit of the allowed range. What is more, Unibest was unable to outperform the neural networks and was only marginally better than the baseline prediction and the long-term mean sandbar location.

Using more than two neighboring partitions for calibration caused a decrease in performance. Increasing the number of calibration partitions often resulted in parameter settings that caused rapid sandbar decay everywhere in the profile (e.g. Figure 3c). Even sandbars that were occasionally generated after the start of a partition quickly disappeared (e.g. Figure 3c in parts 12 and 15). Obviously, sandbar-crest prediction errors increase when the predicted profiles do not contain any sandbars. As can be inferred from Table 1, rapid sandbar decay was achieved by setting α_w close to the upper bound of the allowed range (i.e. $\alpha_w \approx 0.2$ with small standard deviation). The other parameters, k_c and $\tan(\phi)$ varied considerably between different partitions (large standard deviation), but since α_w was large, their exact value did not affect the general behavior much. Apparently, a parameter setting for which Unibest predicts rapid sandbar decay is better than a setting that produces profiles with sandbars, but at the wrong place.

Table 2 shows that using *one* (before or after) neighboring partition for calibration also deteriorated the results. While parameter settings obtained from calibration on a single partition often produced clearly distinguishable sandbars, the predicted offshore migration rate in other partitions was incorrect, resulting in growing errors over time.

To investigate the range of Unibest parameter values required to reproduce observed sandbar behavior in different partitions, we applied the calibration procedure on each partition individually. Optimal parameter settings for each of the 16 partitions are given in Figure 5, and their averages and standard deviations in Table 1. Hindcasts for the partitions on which the parameters were calibrated are given in Figure 3d. For most partitions, the calibration method found parameter settings that produced migrating sandbars, but there were also some partitions for which physically unrealistic parameter settings were found, resulting in profiles without well-developed sandbars (e.g. Figure 3d parts 4, 5, 9 and 15), and causing large standard deviations in the optimal parameter settings (Table 1). The parameters that did produce migrating sandbars were however not clustered in the same region of the parameter space, as becomes clear from Figure 5. This might be partially caused by the interdependence between k_c and α_w. As Figure 5 highlights, large k_c are generally associated with small α_w, and vice versa. Both parameters affect the current-related transport, α_w by affecting the vertical undertow profile and k_c by influencing the concentration profile. Different combinations of α_w and k_c may thus result in similar sandbar behavior.

Table 2. Sandbar-crest performance values for the Unibest and neural network models. Standard deviations over the 16 partitions are given between parentheses, and where convenient, as percentages of the mean values.

	partitions used for calibration / training	RMSE (m)	skill
reference predictions			
Unibest with *Ruessink et al.* [2007] parameters		87 (46%)	-0.32 (0.59)
long-term mean sandbar-crest location	8	52 (42%)	0.07 (0.54)
Unibest with Nelder-Mead calibration			
Unibest	1	61 (46%)	-0.05 (0.56)
Unibest	2	47 (38%)	0.12 (0.46)
Unibest	8	69 (39%)	-0.25 (0.50)
neural networks			
RLARX-C	8	29 (33%)	0.40 (0.34)
RLARX-3P	8	34 (37%)	0.26 (0.46)
hindcast on partition used for calibration / training			
Unibest	1	35 (56%)	0.37 (0.44)
RLARX-C	1	18 (28%)	0.56 (0.28)
RLARX-3P	1	18 (35%)	0.61 (0.24)

The performance values for the partitions on which the Unibest parameters were calibrated are given in Table 2. For comparison Table 2 also shows the results for the neural network models when trained on the (single) hindcasted partition. The positive skill score achieved when Unibest hindcasts the partition on which it was calibrated (Table 2) and the results in Figure 3d indicate that this model is, in principle, able to reproduce observed sandbar behavior for the partition on which it is calibrated. However, Unibest performance remained inferior to the performance of neural networks trained on the hindcasted partition.

4.2. Neural networks

The neural networks were much better at predicting cross-shore sandbar behavior than Unibest. Especially the offshore-directed trends (Figure 4) were reproduced more accurately by both neural network models. As a result, the neural networks were able to outperform the baseline prediction of no change (positive skill scores in Table 2) as well as the long-term mean sandbar location. Although additional profile information was available in RLARX-3P, the predicted migration patterns were very similar and both models often over- and under-predict sandbar locations in the same partitions (Figure 4).

Moreover, the simpler RLARX-C model achieved a higher performance than the more detailed RLARX-3P. A possible reason for this is that the local wave height used in RLARX-C is a better estimate for sandbar migration than the offshore wave height and period data used for RLARX-3P. To investigate whether the different external forcings caused the performance difference between RLARX-3P and RLARX-C, we repeated the experiments with switched forcings (i.e. RLARX-C was trained and tested using offshore wave height and period data, and RLARX-3P with local wave heights only). We found, however, that RLARX-C still outperformed RLARX-3P, even for different forcings. We also found that, independent of the external forcings, both models achieved similar performance on the partition on which the networks were *trained* (see Table 2). This indicates that the performance difference between RLARX-C and RLARX-3P on partitions withheld from training is not generated during training, but arises from the increased generalizing capacity of RLARX-C over RLARX-3P. The only difference between the two neural networks is the number of variables on which the predicted sandbar location depends. In RLARX-3P, the predicted sandbar location not only depends on the previous sandbar location, as in the RLARX-C model, but also on the previous sandbar-crest *elevation* and the previous coordinates of the trough and the sandbar foot. From this we infer that the decreased performance of RLARX-3P compared to RLARX-C is caused by the larger number of parameters to which the predicted sandbar location is sensitive.

4.3. Performance over time

To investigate how the accuracy of the models evolves over time, we evaluated the model performance using the parameters obtained with the optimal number of neighboring partitions (two for Unibest and eight for the neural networks). All models were initialized at the first day of each partition, and iterated forward with observed hydrodynamics, and predicted profiles or sandbar-state variables. Errors were then computed starting from the first prediction to the end of the partition, and averaged over all 16 partitions. Figure 6 shows the average root-mean-squared error in sandbar location as a function of the number of days predicted ahead, for all models. For comparison, Figure 6 also shows the error associated with the long-term (based on eight neighboring partitions) sandbar location. Since only a small number of partitions were longer than 200 days, we could not compute accurate average results for prediction horizons longer than 200 days.

As becomes clear from this figure, the error increases for all models over the first 200 days of prediction. In partitions longer than 200 days, the error usually did not increase further after 200 days, and sometimes even decreased again around prediction horizons of a year. In many partitions, sandbar behavior in the first 200 days is dominated by the offshore-directed trends. Only when the offshore-directed trend becomes less important relative to seasonal behavior (in partitions longer than a year), did the prediction error decrease again. The continuous increase in all prediction errors over the first 200 days indicates that reproducing the offshore-directed trend is difficult for *all* models.

4.4. Profile Predictions

Despite our efforts to find Unibest parameter settings that reproduce observed sandbar behavior, the neural networks achieved better performance than Unibest. However, the comparison between Unibest and the neural networks on their ability to predict sandbar locations might be considered unfair, since the two models were optimized on different performance measures. The neural networks were both optimized and tested on sandbar locations, while Unibest was optimized on profile elevations, but tested on its ability to predict cross-shore sandbar locations. It is however

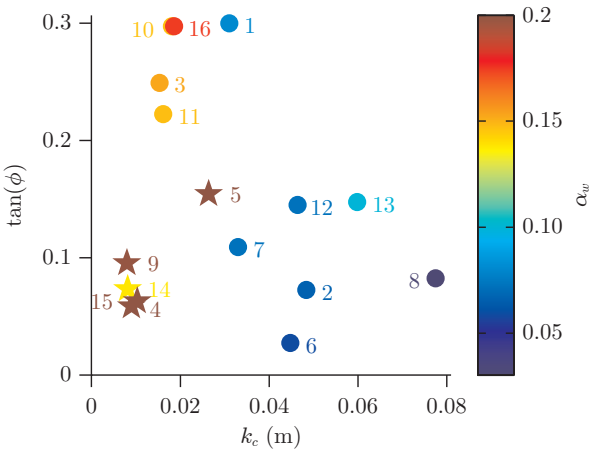

Figure 5. Optimal Unibest parameter values for the current-related roughness k_c (horizontal), the angle of repose tan(ϕ) (vertical) and the vertical eddy viscosity distribution scale factor α_w (color), obtained for each partition (number). Parameter settings resulting in rapid sandbar decay are represented by stars.

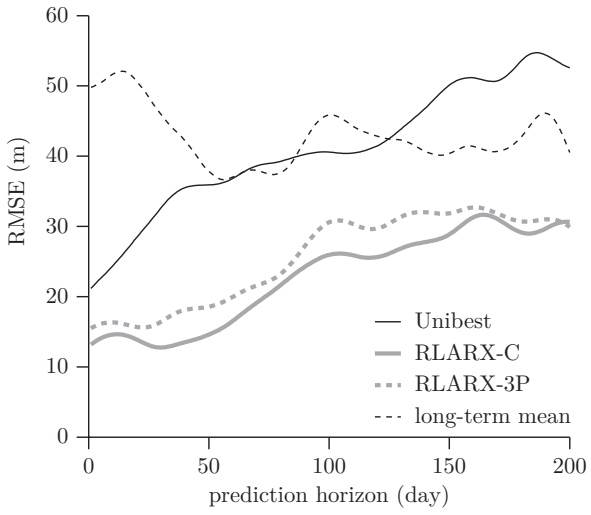

Figure 6. Root-mean-squared prediction error in sandbar-crest location as function of the number of days predicted ahead (prediction horizon), averaged over all 16 partitions. Unibest was calibrated on 2 neighboring partitions, and RLARX-C and RLARX-3P were trained on 8 neighboring partitions.

also possible to compare the performance of Unibest and RLARX-3P on profile elevations (vertical coordinates). For this comparison, we used the three coordinates predicted by the RLARX-3P model together with the long-term mean profile (based on the eight partitions used for training) to construct predicted profiles, in the manner described at the start of this section. Next, we computed the root-mean-squared difference between observed and predicted profile elevations between the 30 and 550 m-coordinate, which loosely covers the part between the trough and sandbar-foot locations (see Figure 2b) and corresponds to the part on which Unibest was calibrated. Additionally, we computed profile-elevation skill scores according to equation 1, using the first profile at the start of each partition as the baseline prediction. Table 3 shows the performance measures over the profiles for both Unibest and RLARX-3P. For comparison, we also included performance measures of merely predicting the long-term (based on eight neighboring partitions) sandbar-less mean profile between the 30 and 550 m-coordinate.

As becomes clear from Tables 2 and 3, the RLARX-3P model not only outperforms Unibest on sandbar locations, but also on profile elevations. Using smaller parts of the profile (i.e. starting further offshore of the 30 m coordinate and onshore of the 550 m coordinate) for the error computation slightly increased the errors, because most of the profile variability is related to the sandbars. However, the RLARX-3P elevation performance remained better than the Unibest elevation performance, even when the error was computed over smaller parts of the profile. What is more, Unibest was not able to outperform a long-term mean profile prediction, while the results of the RLARX-3P model were only slightly better than the long-term mean profile.

5. Discussion

Both the Unibest and neural network models were able to produce several general features of cross-shore sandbar behavior at HORS, such as rapid offshore migration, slower onshore return and net-offshore migration. However, predicting the cross-shore sandbar *location* over prediction horizons of several months to years turned out to be more difficult. The Unibest model produced the least accurate results and could only outperform a no-change prediction when it was allowed to use different parameter settings for different parts of the data. The neural network models, on the other hand, were able to predict sandbar locations more accurately. Moreover, the RLARX-3P outperformed Unibest both on sandbar locations and profile elevations.

The calibration procedure used to find optimal Unibest parameter settings gives several clues about the reason for the inaccurate Unibest results. First, we found that considerably different parameter settings are required to accurately model different parts of the data. Second, a parameter setting that allows for accurate hindcasts of sandbar behavior in one part of the observations, produces highly inaccurate behavior in other parts. Third, when calibration is performed on larger parts of the observations, it turns out to be better to predict profiles *without* sandbars. From these findings we conclude that certain aspects of sandbar behavior can be reproduced by Unibest *within* one data partition, but cannot be generalized to other partitions.

Since the data were divided in partitions of offshore-migration cycles, the most significant aspect of sandbar behavior within one partition is the offshore-directed trend. Unibest parameters obtained from a small part of the observations can be used to reproduce the offshore-directed trend in that part, but yield the wrong trends in other parts of the data. Apparently, the exact *slope* of the offshore-directed trend is very sensitive to the Unibest parameters. When offshore sandbar migration is predicted at the wrong rate, the predicted sandbar crest will end up in the observed trough, or the predicted trough ends up at the observed sandbar-crest location. Predicting sandbars at the wrong location considerably deteriorates predictions of profile *elevations*, both for Unibest and RLARX-3P. When Unibest puts the sandbar in the wrong place, the error in the profile elevation rapidly becomes larger than the mean (sandbar-less) profile. Similarly, errors in the horizontal location of the sandbar-crest, sandbar-foot and trough, result in considerable errors in the vertical elevations in the profiles constructed from

Table 3. Profile-elevation performance values for Unibest and RLARX-3P. Standard deviations over the 16 partitions are given between parentheses, and where convenient, as percentages of the mean values.

	partitions used for calibration / training	RMSE (m)	skill
long-term mean profile	8	0.63 (15%)	0.17 (0.18)
Unibest	2	0.77 (21%)	0.02 (0.22)
RLARX-3P	8	0.61 (24%)	0.19 (0.31)

the RLARX-3P results. While RLARX-3P outperformed Unibest on profile elevations, it performed only slightly better than the long-term mean profile prediction.

As mentioned in Section 1, sandbar behavior might be described in more abstract terms as migration toward a wave-height-dependent equilibrium location. However, if this equilibrium location itself exhibits a long-term trend, or if the timescale on which the sandbar migrates toward the equilibrium location is very large compared to the timescale of the wave variability, errors made in the prediction of sandbar locations will still accumulate exponentially over time [*Pape et al.*, in press]. The problem of error accumulation can therefore not always be entirely solved by representing the behavior of a system on a more abstract level, as in the neural network models used here. While the simplest model (RLARX-C) outperformed all other models, it still had difficulty predicting the exact slope of the offshore-directed trends, as indicated by the growth of the error with increasing prediction horizon (Figure 6). The more detailed RLARX-3P model performed worse than RLARX-C, because the outcome depended on additional parameters. Using nonlinear networks caused an additional decrease in performance, while the most detailed model of the underlying physics (Unibest) performed the worst. Apparently, adding more details to a model causes a decrease in the capacity to predict long-term sandbar behavior.

From these findings we conclude that the nonlinearities in the underlying processes are not canceled out on larger and longer scales, but continue to accumulate over time, making it difficult to predict long-term trends in sandbar location. While the unpredictability related to error accumulation is most obvious in the Unibest modeling effort, the effects of nonlinearity are still present on larger and longer scales. Since long-term trends in sandbar location are not the result of a similar trend in some external forcing pattern, but rather the cumulative result of small differences in onshore and offshore migrations at different timescales, it can be expected that any model that tries to predict net-offshore migration trends in an iterative fashion will suffer from this problem.

It can be argued that the reason for the inferior Unibest performance is that certain processes are missing or are inadequately represented in the model formulation (e.g. Unibest is a wave-averaged model). Similarly, the neural network models might be augmented with more detailed information. In fact, the large range of optimal parameters found in the Unibest calibration runs indicates that the model can compensate for incorrect and missing processes by using different parameter settings at different times [see also *Hsu et al.*, 2006]. Some of these adjustable parameters can be replaced by a more detailed description of the underlying processes, potentially leading to better long-term predictions. For example, *van Rijn* [2007] proposed the use of variable k_c as a function of the hydrodynamic and sediment properties. While adding more detailed descriptions of physical processes would intuitively make a model better and more complete, it does not necessarily yield better long-term predictions. Instead, including more detailed descriptions of physical processes might also aggravate the problem of error accumulation [see for example *Oreskes et al.*, 1994; *Oreskes*, 2003]. This is already plainly illustrated by the neural network results: the simplest RLARX-C model outperformed both the more detailed RLARX-3P model and the *nonlinear* versions of these models.

A previous investigation into the predictability of cross-shore sandbar behavior at HORS by *Ruessink and Kuriyama* [2008] revealed divergence of initially similar states during high-wave conditions, but convergence of initially different states during periods of low waves. From their study on the first 1.5 year of the HORS dataset *Ruessink and Kuriyama* [2008] concluded that sandbar behavior is deterministically forced rather than chaotic. Our findings imply that such conclusions always need to be interpreted in relation to the temporal and spatial scale on which sandbar behavior is studied and modeled. Even if the profiles evolve to similar states during low waves, the much larger and less predictable response during high wave events can still be more significant to the long-term predictability of sandbar behavior.

The rate of net-offshore migration does not only determine where a sandbar is at a certain time, but also when sandbars reach the depth at which they start to decay. As such, the *duration* of cycles of net-offshore migration crucially depends on the net-offshore migration rate. Since predicting the exact rate of net-offshore migration is difficult, the duration of cycles of net-offshore sandbar migration will also be difficult to predict. Predicting sandbar behavior on timescales beyond the duration of a single cycle of net-offshore migration will be even more difficult. Even if a model has positive skill in some parts of the data, predictions will eventually start to run out-of-phase with the observed offshore migration cycles, effectively reducing the model skill below zero.

Our findings imply that successful process-based modeling of cross-shore sandbar behavior on timescales up to several weeks does not guarantee accurate predictions of long-term sandbar behavior. Modeling trends in sandbar behavior as the cumulative result of the underlying short- and small-scale physical processes is prone to error accumulation. This might hamper the comparison between competing models and as such, might pose a challenge for our understanding of long-term sandbar behavior.

6. Conclusion

We investigated the predictability of cross-shore sandbar behavior at HORS with models that operate on different abstraction levels. The models were able to produce several general features of cross-shore sandbar behavior at HORS, but predictions of cross-shore sandbar-crest locations became less accurate with increasing prediction horizon. Especially the slope of the trends in cross-shore sandbar location was difficult to reproduce from given initial sandbar- or profile-state variables and hydrodynamic conditions. More detailed and nonlinear models with more processes and adjustable parameters were less accurate in predicting long-term sandbar behavior. The trends in offshore sandbar migration were found to be highly sensitive to the model parameters, which prevents models to generalize to parts of the data withheld from calibration and training. Furthermore, prediction errors for all models increased over the timescales of the offshore-directed trends. Together, these findings indicate that the nonlinearities in the underlying hydrodynamic and sediment-transport processes are not canceled

out on the larger and longer scale of sandbars, but continue to affect the predictability of long-term trends in sandbar behavior. Error accumulation in the short- and small-scale processes of detailed process-based models might therefore pose a challenge for modeling and understanding long-term trends in sandbar behavior.

Acknowledgments. This work was supported by the Netherlands Organization for Scientific Research (NWO) under contract number 864.04.007. The staff members at HORS are acknowledged for conducting profile measurements even during the most violent typhoons. We thank three anonymous reviewers for their many helpful suggestions.

References

Aagaard, T., R. Davidson-Arnott, G. Greenwood, and J. Nielsen (2004), Sediment supply from shoreface to dunes: linking sediment transport measurements and long-term morphological evolution, *Geomorphology*, *60*, 205–224.

Battjes, J. A., and J. P. F. M. Janssen (1978), Energy loss and set-up due to breaking in random waves, in *Proceedings of the 16th Conference on Coastal Engineering*, pp. 569–587, American Society of Civil Engineering.

Battjes, J. A., and M. J. F. Stive (1985), Calibration and verification of a dissipation model for random breaking waves, *Journal of Geophysical Research*, *90*, 9159–9167.

Bishop, C. M. (1995), *Neural Networks for Pattern Recognition*, Oxford University, New York.

Certain, R., and J. P. Barusseau (2005), Conceptual modelling of sand bars morphodynamics for a microtidal beach (Sète, France), *Bulletin de la Societe Geologique de France*, *176*(4), 343–354.

de Vriend, H. J. (2001), Long-term morphological prediction, in *River, Coastal, and Estuarine Morphodynamics*, pp. 163–190, Springer, Berlin.

De Vriend, H. J., and M. J. F. Stive (1987), Quasi-3d modelling of nearshore currents, *Coastal Engineering*, *11*, 565–602.

Fritsch, F. N., and R. E. Carlson (1980), Monotone piecewise cubic interpolation, *SIAM Journal of Numerical Analysis*, *17*, 238–246.

Gallagher, E. L., S. Elgar, and R. T. Guza (1998), Observations of sand bar evolution on a natural beach, *Journal of Geophysical Research*, *103*, 3203–3215.

Hoefel, F., and S. Elgar (2003), Wave-induced sediment transport and sandbar migration, *Science*, *299*(5614), 1885–1887.

Hornik, M., M. Stinchcombe, and H. White (1989), Multilayer feedforward networks are universal approximators, *Neural Networks*, *2*, 359–366.

Hsu, T. J., S. Elgar, and R. T. Guza (2006), Wave-induced sediment transport and onshore sandbar migration, *Coastal Engineering*, *53*, 817–824.

Kuriyama, Y. (2002), Medium-term bar behavior and associated sediment transport at Hasaki, Japan, *Journal of Geophysical Research*, *107*, 3132.

Kuriyama, Y. (2009), Numerical model for bar migration at Hasaki, Japan, in *Proceedings of Coastal Dynamics*, p. no.50, Tokyo, Japan.

Kuriyama, Y., Y. Ito, and S. Yanagishima (2008), Medium-term variations of bar properties and their linkages with environmental factors at Hasaki, Japan, *Marine Geology*, *248*, 1–10.

Lagarias, J. C., J. A. Reeds, M. H. Wright, and P. E. Wright (1998), Convergence properties of the Nelder-Mead Simplex Method in low dimensions, *SIAM Journal of Optimization*, *9*, 112–147.

Lippmann, T. C., R. A. Holman, and K. K. Hathaway (1993), Episodic, nonstationary behavior of a two sand bar system at Duck, *Journal of Coastal Research*, *15*, 49–75.

Lorenz, E. N. (1963), Deterministic nonperiodic flow, *Journal of the Atmospheric Sciences*, *20*, 130–141.

Oreskes, N. (2003), The role of quantitative models in science, in *The Role of Models in Ecosystem Science*, edited by J. J. C. C. D. Canham and W. K. Laurenroth, pp. 13–31, Princeton University Press, Princeton, New Jersey.

Oreskes, N., K. Shrader-Frechette, and K. Belitz (1994), Verification, validation, and confirmation of numerical models in the Earth sciences, *Science*, *263*, 641–646.

Pape, L., and B. G. Ruessink (2008), Multivariate analysis of nonlinearity in sandbar behavior, *Nonlinear Processes in Geophysics*, *15*, 145–158.

Pape, L., B. G. Ruessink, M. A. Wiering, and I. L. Turner (2007), Recurrent neural network modeling of nearshore sandbar behavior, *Neural Networks*, *20*, 509–518.

Pape, L., N. G. Plant, and B. G. Ruessink (in press), On cross-shore sandbar behavior and equilibrium states, *Journal of Geophysical Research*.

Plant, N. G., R. A. Holman, M. H. Freilich, and W. A. Birkemeier (1999), A simple model for interannual sandbar behavior, *Journal of Geophysical Research*, *104*, 15,755–15,776.

Plant, N. G., M. H. Freilich, and R. A. Holman (2001), Role of morphologic feedback in surf zone sandbar response, *Journal of Geophysical Research*, *106*, 973–989.

Plant, N. G., K. T. Holland, and R. A. Holman (2006), A dynamical attractor governs beach response to storms, *Geophysical Research Letters*, *33*, L17,607.

Reniers, A. J. H. M., E. B. Thornton, T. P. Stanton, and J. A. Roelvink (2004), Vertical flow structure during Sandy Duck: Observations and modeling, *Coastal Engineering*, *51*, 237–260.

Roelvink, J. A., and I. Brøker (1993), Cross-shore profile models, *Coastal Engineering*, *21*, 163–191.

Roelvink, J. A., T. J. G. P. Meijer, K. Houwman, R. Bakker, and R. Spanhoff (1995), Field validation and application of a coastal profile model, in *Proceedings of Coastal Dynamics*, pp. 818–828, American Society of Civil Engineering, New York.

Ruessink, B. G., and Y. Kuriyama (2008), Numerical predictability experiments of cross-shore sandbar migration, *Geophysical Research Letters*, *35*, L01,603.

Ruessink, B. G., K. M. Wijnberg, R. A. Holman, Y. Kuriyama, and I. M. J. van Enckevort (2003), Intersite comparison of interannual nearshore bar behavior, *Journal of Geophysical Research*, *108*, 3249.

Ruessink, B. G., Y. Kuriyama, A. J. H. M. Reniers, J. A. Roelvink, and D. J. R. Walstra (2007), Modeling cross-shore sandbar behavior on the timescale of weeks, *Journal of Geophysical Research*, *112*, F03,010.

Ruessink, B. G., L. Pape, and I. L. Turner (2009), Daily to interannual cross-shore sandbar migration: observations from a multiple sandbar system, *Continental Shelf Research*, *29*, 1663–1677.

Ruggiero, P., G. M. Kaminsky, G. Gelfenbaum, and B. Voigt (2005), Seasonal to interannual morphodynamics along a high-energy dissipative littoral cell, *Journal of Coastal Research*, *21*(3), 553–578.

Rumelhart, D., G. Hinton, and R. Williams (1986), Learning internal representations by error propagation, *Parallel Distributed Processing*, *1*, 318–362.

van Enckevort, I. M. J., and B. G. Ruessink (2003), Video observations of nearshore bar behaviour. Part 1: alongshore uniform variability, *Continental Shelf Research*, *23*, 501–512.

van Rijn, L. C. (1993), *Principles of Sediment Transport in Rivers, Estuaries and Coastal Seas*, Aqua Publications, Blokzijl, The Netherlands.

van Rijn, L. C. (2007), Unified view of sediment transport by currents and waves. I: initiation of motion, bed roughness, and bed-load transport, *Journal of Hydraulic Engineering*, *133*, 649–667.

Werner, B. T. (1999), Complexity in natural landform patterns, *Science*, *284*, 102–104.

Werner, B. T. (2003), Modeling landforms as self-organized, hierarchical dynamical systems, in *Prediction in Geomorphology*, Geophysical Monograph 135, pp. 133–150, AGU Press.

Wijnberg, K. M., and J. H. J. Terwindt (1995), Extracting decadal morphological behaviour from high-resolution, long-term bathymetric surveys along the Holland coast using eigenfunction analysis, *Marine Geology*, *126*, 301–330.

Williams, R. J., and J. Peng (1990), An efficient gradient-based algorithm for on-line training of recurrent network trajectories, *Neural Computation*, *2*, 490–501.

L. Pape, IDSIA (Istituto Dalle Molle di Studi sull'Intelligenza Artificiale), Galleria 2, 6928 Manno-Lugano, Switzerland (pape@idsia.ch)

Y. Kuriyama, Marine Environment and Engineering Department, Port and Airport Research Institute, Nagase 3-1-1, Yokosuka, Kanagawa 239-0826, Japan. (kuriyama@pari.go.jp)

B. G. Ruessink, Faculty of Geosciences, Department of Physical Geography, Universiteit Utrecht, Heidelberglaan 2, 3584 CS Utrecht, The Netherlands. (g.ruessink@geo.uu.nl)